NeuroImage: Clinical 38 (2023) 103394

Contents lists available at ScienceDirect

NeuroImage: Clinical

journal homepage: www.elsevier.com/locate/ynicl

Spatial patterns of elevated magnetic susceptibility in progressive apraxia of speech

Ryota Satoh [a], Arvin Arani [b], Matthew L. Senjem [b,c], Joseph R. Duffy [a], Heather M. Clark [a], Rene L. Utianski [a], Hugo Botha [a], Mary M. Machulda [d], Clifford R. Jack Jr [b], Jennifer L. Whitwell [b], Keith A. Josephs [a,*]

[a] Department of Neurology, Mayo Clinic, Rochester, MN, USA
[b] Department of Radiology, Mayo Clinic, Rochester, MN, USA
[c] Department of Information Technology, Mayo Clinic, Rochester, MN, USA
[d] Department of Psychiatry and Psychology, Mayo Clinic, Rochester, MN, USA

ARTICLE INFO

Keywords:
Apraxia of speech
Progressive apraxia of speech
Magnetic resonance imaging
Quantitative susceptibility mapping
Iron

ABSTRACT

Purpose: Progressive apraxia of speech (PAOS) is a neurodegenerative disorder affecting the planning or programming of speech. Little is known about its magnetic susceptibility profiles indicative of biological processes such as iron deposition and demyelination. This study aims to clarify (1) the pattern of susceptibility in PAOS patients, (2) the susceptibility differences between the phonetic (characterized by predominance of distorted sound substitutions and additions) and prosodic (characterized by predominance of slow speech rate and segmentation) subtypes of PAOS, and (3) the relationships between susceptibility and symptom severity.

Methods: Twenty patients with PAOS (nine phonetic and eleven prosodic subtypes) were prospectively recruited and underwent a 3 Tesla MRI scan. They also underwent detailed speech, language, and neurological evaluations. Quantitative susceptibility maps (QSM) were reconstructed from multi-echo gradient echo MRI images. Region of interest analysis was conducted to estimate susceptibility coefficients in several subcortical and frontal regions. We compared susceptibility values between PAOS and an age-matched control group and performed a correlation analysis between susceptibilities and an apraxia of speech rating scale (ASRS) phonetic and prosodic feature ratings.

Results: The magnetic susceptibility of PAOS was statistically greater than that of controls in subcortical regions (left putamen, left red nucleus, and right dentate nucleus) ($p < 0.01$, also survived FDR correction) and in the left white-matter precentral gyrus ($p < 0.05$, but not survived FDR correction). The prosodic patients showed greater susceptibilities than controls in these subcortical and precentral regions. The susceptibility in the left red nucleus and in the left precentral gyrus correlated with the prosodic sub-score of the ASRS.

Conclusion: Magnetic susceptibility in PAOS patients was greater than controls mainly in the subcortical regions. While larger samples are needed before QSM is considered ready for clinical differential diagnosis, the present study contributes to our understanding of magnetic susceptibility changes and the pathophysiology of PAOS.

Abbreviations: AOS, apraxia of speech; ASRS-3, Apraxia of Speech Rating Scale- version 3; BNT, Boston Naming Test Short Form; CBD, corticobasal degeneration; CBS, corticobasal syndrome; FAB, Frontal Assessment Battery; FDR, false discovery rate; GM, gray matter; MCALT, Mayo Clinic Adult Lifespan Template; MDS-UPDRS III, Movement Disorders Society-sponsored revision of the Unified Parkinson's Disease Rating Scale Part III; MoCA, Montreal Cognitive Assessment; MPRAGE, magnetization prepared rapid acquisition gradient echo; NVOA, nonverbal oral apraxia scale; PAOS, progressive apraxia of speech; PPAOS, primary progressive apraxia of speech; PSP, progressive supranuclear palsy; QSM, quantitative susceptibility mapping; ROI, regions of interest; WM, white matter; WAB AQ, Western Aphasia Battery Aphasia Quotient.

* Corresponding author at: Neurology and Neuroscience, Ani Professor of Alzheimer's Disease Research, Mayo Clinic, College of Medicine and Science, 200 1st Street S.W., Rochester, MN 55905, USA.

E-mail address: josephs.keith@mayo.edu (K.A. Josephs).

https://doi.org/10.1016/j.nicl.2023.103394
Received 19 January 2023; Received in revised form 23 March 2023; Accepted 27 March 2023
Available online 28 March 2023

1. Introduction

Apraxia of speech (AOS) is a motor speech disorder affecting the planning or programming of speech. While AOS can result from left hemisphere stroke, it can also be a symptom of neurodegenerative disease where it is referred to as progressive apraxia of speech (PAOS) (Duffy and Josephs, 2012). PAOS is strongly associated with a 4-repeat tauopathy with the underlying pathology of progressive supranuclear palsy (PSP) or corticobasal degeneration (CBD) (Josephs et al., 2021; Josephs et al., 2006). Apraxia of speech can be the sole presenting feature of PAOS (referred to as primary progressive apraxia of speech, or PPAOS) (Josephs et al., 2012) or PAOS patients can present with both AOS and agrammatic aphasia in which case they may also meet criteria for the non-fluent/ agrammatic variant of primary progressive aphasia (Gorno-Tempini et al., 2011). Most PAOS patients eventually develop clinical features of PSP or corticobasal syndrome (CBS) (Josephs et al., 2014; Seckin et al., 2020). Interestingly, the underlying pathology is also associated with two clinically distinguishable PAOS subtypes called phonetic (characterized by predominance of distorted sound substitutions and additions) and prosodic (characterized by predominance of slow speech rate and segmentation) (Utianski et al., 2018a); phonetic PAOS is more often associated with CBD while prosodic PAOS is more often associated with PSP (Josephs et al., 2021).

Over the past couple of decades, neuroimaging studies have assessed patterns of neurodegeneration in patients with PAOS. The involvement of supplementary motor area and premotor cortex have been detected as gray-matter (GM) and white-matter (WM) atrophy on structural MRI, WM degeneration on diffusion tensor imaging, and hypometabolism on [18F] fluorodeoxyglucose PET in patients with PPAOS (Josephs et al., 2013; Josephs et al., 2012). The additional involvement of Broca's area and WM tracts connecting to Broca's area have been observed in patients with concomitant agrammatic aphasia (Catani et al., 2013; Gorno-Tempini et al., 2004; Josephs et al., 2013; Valls Carbo et al., 2022). Atrophy in subcortical regions, including basal ganglia and midbrain, have also been observed (Josephs et al., 2021; Josephs et al., 2014; Josephs et al., 2006; Whitwell et al., 2013a). Recent studies also reveal that these regions are differentially affected between phonetic and prosodic subtypes (Utianski et al., 2018a) and largely overlap with regions affected in PSP (Whitwell et al., 2013a) and CBD, reflecting the associations with underlying pathology (Josephs et al., 2021; Josephs et al., 2006).

Quantitative susceptibility mapping (QSM) is a relatively new MRI technique to estimate the magnetic susceptibilities of biological tissues (Wang and Liu, 2015). The tissues include paramagnetic substances (positive susceptibility coefficients) like iron-containing molecules and diamagnetic substances (negative susceptibility coefficients) like myelin lipids (Liu et al., 2015). Hence, QSM can detect abnormal deposition or loss of these substances associated with several diseases (Wang et al., 2017). QSM has played an important role in the better understanding of neurodegenerative diseases as it provides novel insights on abnormal iron deposition or demyelination associated with degeneration (Ravanfar et al., 2021). Indeed, many studies on Alzheimer's disease (Acosta-Cabronero et al., 2013; Kim et al., 2017), Parkinson's disease (Acosta-Cabronero et al., 2017; Guan et al., 2019), and PSP (Sjostrom et al., 2017) have demonstrated susceptibility increases in several subcortical and cortical regions. Considering the large amount of cortical damage in CBD (Josephs et al., 2008) and subcortical iron deposition in PSP (Ravanfar et al., 2021), we would expect susceptibility to also increase in several brain regions of PAOS patients. However, to our knowledge no studies have accessed susceptibility changes in PAOS patients or the relationship between susceptibility and AOS severity in PAOS.

This study assessed brain susceptibility patterns in PAOS patients by using QSM. Our hypothesis is that susceptibility is increased in several subcortical and cortical regions. To address our aims, we examined (1) the regions of greater susceptibility in PAOS patients than controls, (2) the susceptibility difference between phonetic and prosodic subtypes in the extracted regions, and (3) the relationships between susceptibility and AOS feature severity.

2. Methods

2.1. Participants

Twenty patients diagnosed with PAOS (nine with the phonetic and eleven with the prosodic subtype) were prospectively recruited by the Mayo Clinic, Neurodegenerative Research Group (NRG), between July 2020 and March 2022 (Josephs et al., 2013). They underwent detailed speech, language, and neurological evaluations, and a 3 Tesla (3-T) MRI scan. The speech and language evaluation included the Apraxia of Speech Rating Scale- version 3 (ASRS-3) and its phonetic and prosodic sub-scores (Strand et al., 2014; Utianski et al., 2018a), the Western Aphasia Battery Aphasia Quotient (WAB AQ) (Kertesz, 2007), the Boston Naming Test Short Form (BNT) (Lansing et al., 1999), and a nonverbal oral apraxia scale (NVOA) (Botha et al., 2014). The neurological evaluation included the Montreal Cognitive Assessment (MoCA) (Nasreddine et al., 2005), the Frontal Assessment Battery (FAB) (Dubois et al., 2000), the Movement Disorders Society-sponsored revision of the Unified Parkinson's Disease Rating Scale Part III (MDS-UPDRS III) (Goetz et al., 2008), PSP rating scale (Golbe and Ohman-Strickland, 2007), and PSP Saccadic Impairment Scale (PSIS) (Whitwell et al., 2011). Sixty-seven cognitively normal participants (48 females) who did not have any complaints of cognitive, motor, or behavioral abnormalities and met the criteria of MoCA $\geq$ 23 (Carson et al., 2018) were also recruited by NRG over approximately the same time period, and underwent the same MRI scans. The median MoCA score in the controls was 27 (standard deviation: 1.7).

2.2. MRI protocol

All participants underwent a standardized MRI protocol on closed-bore 3-T scanners (Magnetom Prisma, Siemens AG, Healthineers, Erlangen, Germany). A 3D Magnetization Prepared Rapid Acquisition Gradient-Echo (MPRAGE) was acquired with TR of 2300 ms, TE of 3 ms, T1 of 945 ms, flip angle of 9°, and 0.8 mm isotropic resolution. For QSM analysis, 3D multi-echo gradient echo sequence was acquired with TR of 28.0 ms, TE of 6.7, 10.6, 14.5, 18.4, and 22.4 ms, flip angle of 15°, a 20-cm field of view, acquisition in-plane matrix of 384 $\times$ 269, slice number of 88, slice thickness of 1.8 mm, GRAPPA acceleration factor (phase-encode direction) of 2.0, and scan time of 6 min 37 s.

2.3. Image processing

The T1-weighted images from the MPRAGE scan were segmented into GM and WM using the templates and settings from the Mayo Clinic Adult Lifespan Template (MCALT: https://www.nitrc.org/projects/mcalt/). Atlases for several regions of interest (ROIs) were nonlinearly registered from MCALT space to each subject space using Advanced Normalization Tools (ANTs: https://stnava.github.io/ANTs/). The QSM images were reconstructed from the multi-echo gradient echo images using MATLAB (The MathWorks Inc., Natick, Massachusetts, USA) and STI suite (https://people.eecs.berkeley.edu/~chunlei.liu/software.html). The reconstruction process includes a Laplacian-based method to unwrap each phase image (Schofield and Zhu, 2003), phase summing to combine all-echo unwrapped phase images (Chen et al., 2021), variable-kernel sophisticated harmonic artifact reduction for phase data method (Wu et al., 2012) for background field removal, and iterative least squares decomposition method (Li et al., 2015) for dipole inversion. The reconstructed QSM images were then rigidly registered to the T1 weighted images from the MPRAGE scan using statistical parametric mapping (SPM12: https://www.fil.ion.ucl.ac.uk/spm/software/spm12/) to apply the atlases for QSM images.

The susceptibility values were obtained in left and right subcortical

and frontal ROIs using the brain atlases. The ROIs were selected based on the many neuroimaging studies that have reported abnormalities in PAOS in the subcortical and frontal regions (Josephs et al., 2021; Josephs et al., 2013; Josephs et al., 2012; Josephs et al., 2006; Utianski et al., 2018b; Whitwell et al., 2013b). The eight subcortical ROIs were defined in the basal ganglia (caudate, putamen, pallidum, and subthalamic nucleus), thalamus, midbrain (substantia nigra and red nucleus), and cerebellar dentate. The 12 frontal ROIs included the precentral gyrus, superior frontal gyrus (dorsolateral), superior frontal gyrus (orbital part), middle frontal gyrus, middle frontal gyrus (orbital part), inferior frontal gyrus (opercular part), inferior frontal gyrus (triangular part), inferior frontal gyrus (orbital part), rolandic operculum, supplementary motor area, superior frontal gyrus (medial), and superior frontal gyrus (medial orbital). GM and WM were separated in each frontal ROI because they have different compositions of magnetic susceptibility sources in cortex (Stuber et al., 2014). The MCALT atlas (originally from the automated anatomical labeling atlas (Tzourio-Mazoyer et al., 2002)) was used for four subcortical (caudate, putamen, pallidum, and thalamus) and all frontal ROIs; the Deep Brain Stimulation Intrinsic Template atlas (Ewert et al., 2018) for three subcortical ROIs (subthalamic nucleus, substantia nigra, and red nucleus); and an in-house developed atlas (Whitwell et al., 2017) for cerebellar dentate ROI. The susceptibilities in each subcortical ROI were averaged in summed regions of GM and WM masks, and the susceptibilities in each frontal ROI were separately averaged in GM and WM masks respectively. The total number of ROIs was 64 including the left and right subcortical ROIs (2×8) and the left and right and GM and WM masked frontal ROIs ($2 \times 2 \times 12$).

2.4. Statistical analysis

To correct for the influence of normal aging on susceptibility (Acosta-Cabronero et al., 2016), susceptibility in each ROI was converted to the W-score. The conversion process included (1) linear regressions in the control group ($n = 67$) to obtain slopes, intercepts, and residuals, and (2) application of the linear model to all participants' susceptibility values (χ) by using the following equation.

$$W = \frac{\chi - (\alpha \bullet \mathrm{age} + \beta)}{\sigma},$$

where α, β, and σ were the slope, intercept, and standard deviation of residuals of the linear model. The obtained W-scores were interpreted as age-corrected normalized susceptibility values. All 67 controls were used to obtain the linear model to estimate the age effects as accurately as possible, while 19 controls were selected from the 67 to make comparisons between controls and patients with matched age.

To extract the regions with elevated susceptibility of the PAOS patients, Mann-Whitney U test was used to compare susceptibility in each ROI between the PAOS ($n = 20$) and the age-matched control ($n = 19$) groups. A false discovery rate (FDR) test (Benjamini and Hochberg, 1995) was then applied to correct for the multiple comparisons of the 64 ROIs. Then, Dunn's test with Bonferroni correction was used to compare among three groups (control, phonetic, and prosodic groups) in the ROIs where susceptibility was greater in PAOS. Finally, Pearson's correlation coefficients were calculated for the PAOS group to assess the relationship between susceptibilities and AOS severity (phonetic sub-score, prosodic sub-score, and total score of the ASRS-3). The categorical variables in the demographic table (sex, handedness, and number of aphasia present) were compared between any two groups using Fisher's exact test. The continuous variables in the demographic table were compared between any two groups using Mann-Whitney U test. All statistical analyses except for Dunn's test were conducted by using MATLAB Statistics and Machine Learning Toolbox (The MathWorks Inc., Natick, Massachusetts, USA, https://www.mathworks.com/help/stats/). Dunn's test was performed by using R software.

This study was approved by the Mayo Clinic Institutional Review Board, and informed consent was obtained from all participants.

3. Results

The demographic features are shown in Table 1. There were no significant differences in sex, education, age, or handedness between the PAOS and control groups. Regarding the comparison of phonetic and prosodic groups, there were no significant differences in sex, education, handedness, age at MRI scan, age at disease onset, or disease duration. There were also no significant differences between the subtypes in MoCA, FAB, MDS-UPDRS III, PSP rating scale, PSIS, ASRS-3 total score, WAB AQ, BNT, or NVOA scores. Aphasia was present in 6 out of the 9

Table 1
Demographics and clinical findings for phonetic and prosodic subtypes of PAOS and age-matched control group.

	Phonetic (n = 9)	Prosodic (n = 11)	Control (n = 19)	P-value (PAOS vs. control)	P –value (phonetic vs. prosodic)
Female, n (%)	3 (33%)	7 (64%)	9 (47%)	1.00	0.37
Education, y	16 (16, 18)	18 (15, 18)	16 (15, 18)	0.59	0.84
Handedness, Left (%)	0 (0%)	2 (18%)	3 (16%)	0.66	0.48
Age at scan, y	68 (61, 75)	75 (71, 79)	70 (66, 74)	0.22	0.16
Age at onset, y	66 (57, 70)	71 (67, 74)			0.11
Disease duration from onset to scan, y	3.8 (2.4, 6.6)	4.3 (2.6, 5.2)			0.97
MoCA (/30)	21 (16, 23)	24 (20, 27)	26 (25, 27)	<0.01	0.12
FAB (/18)	16 (15, 17)	14 (13, 17) [a]			0.53
MDS-UPDRS III (/132)	11 (7, 20)	15 (12, 20)			0.42
PSP rating scale (/100)	12 (6, 18)	14 (8, 17) [b]			0.76
PSIS (/5)	1 (0, 1)	1 (0, 1) [b]			0.89
Aphasia present, yes (%)	6 (67%)	6 (55%)			0.67
AOS severity (/4)	2 (1.5, 2.5)	2 (1, 3)			1.00
ASRS-3 total score (/52)	22 (17, 29)	23 (15, 31)			0.85
ASRS-3 phonetic sub-score	9 (7, 14)	6 (3, 8)			<0.05
ASRS-3 prosodic sub-score	6 (3, 8)	10 (6, 13)			<0.05
WAB AQ (/100)	83.9 (75.7, 98.6)	97.2 (93.0, 98.6)			0.12
BNT (/15)	13 (12, 15)	15 (13, 15)			0.33
NVOA (/32)	27 (18, 31)	27 (23, 29)			0.85

Results are shown as median (first and third quartiles) for all continuous values. [a] FAB was evaluated on nine prosodic patients. [b] PSP rating scale and PSIS were evaluated on ten prosodic patients.
Abbreviations: MoCA = Montreal Cognitive Assessment; FAB = Frontal Assessment Battery; MDS-UPDRS III = Movement Disorders Society-sponsored revision of the Unified Parkinson's Disease Rating Scale Part III; PSP = Progressive supranuclear palsy; PSIS = PSP Saccadic Impairment Scale; AOS = Apraxia of speech; ASRS = Apraxia of Speech Rating Scale; WAB AQ = Western Aphasia Battery Aphasia Quotient; BNT = Boston Naming Test Short Form; NVOA = nonverbal oral apraxia scale.

patients in the phonetic group and 6 out of the 11 patients in the prosodic group ($p = 0.67$). As expected, the ASRS-3 phonetic and prosodic sub-scores differed between two subtypes ($p < 0.05$).

Table 2 shows the regions with greater susceptibility in PAOS compared to controls ($p < 0.05$). The p-values were calculated by Mann-Whitney U test, and the asterisks in Table 2 show the regions that survived FDR correction (FDR < 0.05). In the subcortical regions, the left putamen, left subthalamic nucleus, bilateral substantia nigra, bilateral red nucleus, and bilateral cerebellar dentate showed greater susceptibility in PAOS compared to controls. In the frontal regions, no ROIs were identified for the GM mask, and one ROI (left precentral gyrus) was identified for the WM mask with greater susceptibilities in PAOS compared to controls. Among these regions, three subcortical ROIs (left putamen, left red nucleus, and right cerebellar dentate) were significant after FDR correction. These results overall showed that PAOS had greater susceptibility in the subcortical regions than controls. The corrected p-values for all 64 ROIs were shown in the Supplementary table.

Boxplots comparing susceptibilities among phonetic, prosodic and control groups in the three subcortical ROIs that showed greater susceptibility to PAOS are shown in Fig. 1(a). Boxplots in the left precentral gyrus are also shown in Fig. 1(b). The corresponding W-scores in each group and p-values in pairwise comparison are shown in Table 3. In the three subcortical regions (left putamen, left red nucleus, and right cerebellar dentate, Fig. 1(a)), median susceptibility values were in the descending order of prosodic, phonetic, and control groups. In these regions, there were significant differences between prosodic and controls ($p < 0.01$) but not between phonetic and controls. In the left precentral gyrus (Fig. 1(b)), the prosodic group susceptibility was greater than controls ($p < 0.05$), but there were no significant differences between control and phonetic groups and phonetic and prosodic groups.

Table 4 shows Pearson's correlation coefficients between susceptibilities and ASRS-3 (phonetic sub-score, prosodic sub-score, and total score). As shown in Table 4 and Fig. 2, the left red nucleus showed a positive correlation between susceptibility and prosodic sub-scores ($r = 0.50$, $p < 0.05$), with greater susceptibility associated with greater prosodic speech disturbance severity. The left WM precentral gyrus also showed a positive correlation between susceptibility and prosodic sub-scores ($r = 0.47$, $p < 0.05$) and between susceptibility and total scores ($r = 0.49$, $p < 0.05$). There were no significant correlations between any susceptibility measure and phonetic sub-scores (Table 4).

4. Discussion

In this study, we examined the spatial pattern of greater magnetic susceptibility in patients with PAOS than controls using QSM. We found greater susceptibility coefficients in subcortical regions (putamen, red nucleus, and cerebellar dentate) and left precentral WM, although only the subcortical regions survived correction for multiple comparisons. These results are topographically similar to those in previous studies using structural MRI, tractography, and FDG-PET (Josephs et al., 2021; Josephs et al., 2012; Josephs et al., 2006; Utianski et al., 2018a), further supporting the idea that PAOS is associated with involvement of the premotor cortex and subcortical regions.

There are several explanations for the causes of greater susceptibility in the subcortical and precentral WM regions (Wang et al., 2017). Given that many histological studies have shown that subcortical susceptibility is strongly linked to iron concentration (Langkammer et al., 2012; Sun et al., 2015), greater susceptibility likely reflects abnormal iron deposition in the subcortical regions. In the precentral WM, both iron deposition and demyelination are the main possible causes of greater susceptibility (Ravanfar et al., 2021). Given that the fractional anisotropy is reduced in this same region in PAOS patients (Josephs et al., 2013; Josephs et al., 2012; Whitwell et al., 2013a), demyelination is presumably one of the factors contributing to the greater susceptibility (Liu et al., 2011). In summary, our results suggest that PAOS is associated with abnormal iron deposition in the midbrain, basal ganglia, and dentate nucleus, and demyelination in the precentral WM. Further studies including histological validation will be needed to confirm these hypotheses.

In the subcortical regions, susceptibility values were in the descending order of prosodic, phonetic, and control groups. Given that the prosodic subtype is more often associated with PSP (Josephs et al., 2021) and that PSP has greater susceptibility in the subcortical regions (Mazzucchi et al., 2022; Sjostrom et al., 2017; Sjostrom et al., 2019), our results may reflect the magnetic susceptibility changes of the underlying pathology. For the correlation analysis, the susceptibilities in the left red nucleus were correlated with the prosodic sub-scores of ASRS-3. The left precentral gyrus was also correlated with the prosodic sub-scores. Interestingly, the red nucleus is the region where susceptibility prominently increases in PSP (Mazzucchi et al., 2022), and the precentral gyrus is the region where atrophy in PAOS and PSP characteristically coincide (Whitwell et al., 2013a). Therefore, the results of the correlation analysis suggest that the commonly affected regions in PSP and prosodic patients are associated with the worsening of prosodic symptoms.

The three subcortical ROIs that survived the FDR correction in the PAOS group were the putamen, red nucleus, and cerebellar dentate. The putamen is connected to the supplementary motor area, the central area in PAOS, and we previously showed that this WM connection correlated to AOS severity (Valls Carbo et al., 2022). The present results again suggest that the putamen is affected in PAOS. The red nucleus is involved in motor control with input from the cerebellum and motor cortex. Additionally, a few MRI studies have shown that it is also involved in speech production (Soros et al., 2006) and developmental stuttering (Watkins et al., 2008). The results of our correlation analysis indicate that degeneration of the red nucleus was related to severity of prosodic symptoms, although the underlying mechanisms are uncertain. The cerebellar dentate showed strong evidence ($p < 0.01$) of higher susceptibility in prosodic patients. This finding is consistent with the previous study (Josephs et al., 2021) showing that the baseline and rate of atrophy in the cerebellar dentate is greater in PAOS-PSP than in PAOS-CBS patients. In the frontal regions, however, only one ROI was identified with greater susceptibilities in PAOS, and we did not observe significant differences in the supplementary motor area although this region is consistently associated with PAOS. This may indicate that changes in iron or demyelination in these areas were relatively small and therefore not detectable. This may also be related to the relatively small dynamic range of susceptibility in the cortex (Cogswell et al., 2021). Although the cause of this discrepancy requires further investigation, it suggests that QSM is better suited to assess abnormalities in subcortical structures in PAOS.

The strengths of the present study are the novelty of studying PAOS using QSM and the careful evaluations and diagnosis of PAOS based on detailed clinical and comprehensive biomarkers. There were also some limitations to this study. First, the numbers of phonetic and prosodic patients were relatively small which may have influenced results of statistical comparisons between the phonetic and prosodic groups.

Table 2
The regions with greater age-corrected susceptibility (W-score) in PAOS patients compared with controls ($p < 0.05$). The p-values were calculated by Mann-Whitney U test. Asterisks (*) shows the regions that survived FDR correction.

Area	Region	P-value
Basal ganglia	Left putamen	<0.01*
	Left subthalamic nucleus	0.05
Midbrain	Left substantia nigra	<0.01
	Right substantia nigra	0.05
	Left red nucleus	<0.01*
	Right red nucleus	0.02
Cerebellar	Left cerebellar dentate	0.02
	Right cerebellar dentate	<0.01*
Frontal lobe (WM)	Left precentral gyrus	0.02

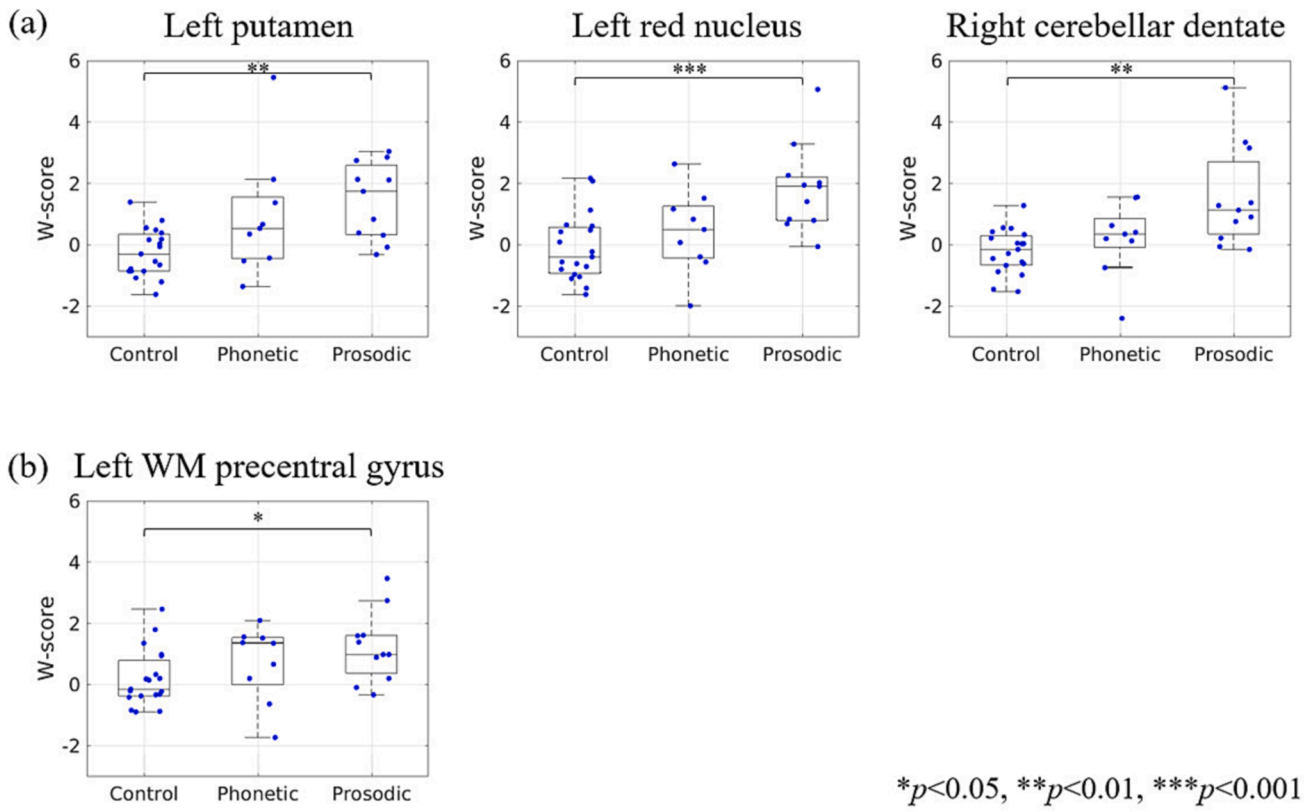

Fig. 1. The age-corrected susceptibilities (W-score) of phonetic subtypes, prosodic subtypes, and controls in the (a) subcortical and (b) WM precentral ROIs. In each boxplot, the center line shows the median, the box shows the interquartile range, and the whiskers extend to the minimum and maximum values except for outliers. The p-values were calculated by using the Dunn's test with Bonferroni correction.

Table 3
The comparison results among control, phonetic, and prosodic groups. W-scores (medians and interquartile ranges) and p-values for each pairwise comparison are shown in the three subcortical regions and one frontal region.

Area	Region	Control	Phonetic	Prosodic	*p* (control vs phonetic)	*p* (control vs prosodic)	*p* (phonetic vs prosodic)
Basal ganglia	Left putamen	−0.29 (−0.85, 0.34)	0.53 (−0.45, 1.56)	1.74 (0.33, 2.59)	0.11	<0.01	0.38
Midbrain	Left red nucleus	−0.39 (−0.93, 0.57)	0.50 (−0.43, 1.25)	1.91 (0.80, 2.20)	0.31	<0.001	0.10
Cerebellar	Right cerebellar dentate	−0.16 (−0.65, 0.30)	0.34 (−0.08, 0.86)	1.12 (0.35, 2.71)	0.21	<0.01	0.19
Frontal WM	Left precentral gyrus	−0.16 (−0.37, 0.79)	1.36 (−0.01, 1.53)	0.98 (0.37, 1.61)	0.21	<0.05	0.73

Table 4
Pearson's correlation coefficients between age-corrected susceptibility (W-score) and apraxia of speech rating scale (phonetic sub-score, prosodic sub-score, and total score) in PAOS patients ($n = 20$).

Area	Region	Phonetic sub-score	Prosodic sub-score	Total score
Basal ganglia	Left putamen	0.06	−0.01	0.02
Midbrain	Left red nucleus	−0.06	0.50*	0.26
Cerebellar	Right cerebellar dentate	−0.27	0.26	−0.03
Frontal WM	Left precentral gyrus	0.25	0.47*	0.49*

*$p < 0.05$.

Second, this study did not address individual patterns, but rather group level differences. Finally, susceptibility anisotropy in WM was not analyzed in this study. WM susceptibility when calculated as the scalar value may be affected by the fiber orientation (Lancione et al., 2017; Sibgatulin et al., 2021). Correcting for these effects using multiple acquisitions or diffusion methods may improve accuracy of WM susceptibility estimation.

In conclusion, the results from this study show that magnetic susceptibility was greater in PAOS patients than controls mainly in the subcortical regions. These regions are qualitatively consistent with those detected in previous neuroimaging studies, supporting previous findings of subcortical damage. The results also show that greater susceptibility in these subcortical regions was more strongly related to the prosodic than phonetic subtype. While a larger sample is required before QSM is considered ready for clinical differential diagnosis, the present study contributes to our understanding of magnetic susceptibility changes and the pathophysiology of PAOS.

CRediT authorship contribution statement

Ryota Satoh: Formal analysis, Investigation, Methodology, Writing

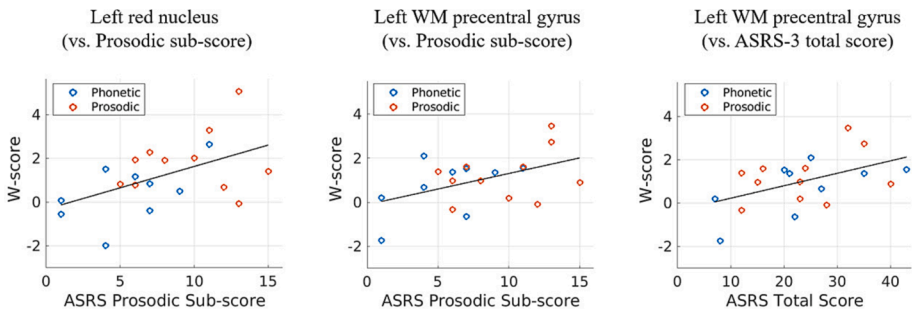

Fig. 2. Relationships between age-corrected susceptibility (W-score) and ASRS-3 scores. Blue and red circles show each patient of phonetic and prosodic subtypes, respectively. (For interpretation of the references to colour in this figure legend, the reader is referred to the web version of this article.)

– original draft. **Arvin Arani:** Methodology, Writing – review & editing. **Matthew L. Senjem:** Methodology, Writing – review & editing. **Joseph R. Duffy:** Resources, Writing – review & editing. **Heather M. Clark:** Resources, Writing – review & editing. **Rene L. Utianski:** Resources, Writing – review & editing. **Hugo Botha:** Resources, Writing – review & editing. **Mary M. Machulda:** Resources, Writing – review & editing. **Clifford R. Jack:** Resources, Methodology, Writing – review & editing. **Jennifer L. Whitwell:** Conceptualization, Methodology, Supervision, Funding acquisition, Writing – review & editing. **Keith A. Josephs:** Conceptualization, Methodology, Resources, Supervision, Funding acquisition, Writing – review & editing.

Declaration of Competing Interest

The authors declare that they have no known competing financial interests or personal relationships that could have appeared to influence the work reported in this paper.

Data availability

The data that has been used is confidential.

Acknowledgement

The study was funded by National Institutes of Health grants R01-DC14942, R01-DC12519 and R01-DC010367.

Appendix A. Supplementary data

Supplementary data to this article can be found online at https://doi.org/10.1016/j.nicl.2023.103394.

References

Acosta-Cabronero, J., Williams, G.B., Cardenas-Blanco, A., Arnold, R.J., Lupson, V., Nestor, P.J., 2013. In vivo quantitative susceptibility mapping (QSM) in Alzheimer's disease. PLoS One 8, e81093.

Acosta-Cabronero, J., Betts, M.J., Cardenas-Blanco, A., Yang, S., Nestor, P.J., 2016. In vivo MRI mapping of brain iron deposition across the adult lifespan. J. Neurosci. 36, 364–374.

Acosta-Cabronero, J., Cardenas-Blanco, A., Betts, M.J., Butryn, M., Valdes-Herrera, J.P., Galazky, I., Nestor, P.J., 2017. The whole-brain pattern of magnetic susceptibility perturbations in Parkinson's disease. Brain 140, 118–131.

Benjamini, Y., Hochberg, Y., 1995. Controlling the false discovery rate: A practical and powerful approach to multiple testing. J. R. Stat. Soc. B. Methodol. 57, 289–300.

Botha, H., Duffy, J.R., Strand, E.A., Machulda, M.M., Whitwell, J.L., Josephs, K.A., 2014. Nonverbal oral apraxia in primary progressive aphasia and apraxia of speech. Neurology 82, 1729–1735.

Carson, N., Leach, L., Murphy, K.J., 2018. A re-examination of Montreal Cognitive Assessment (MoCA) cutoff scores. Int. J. Geriatr. Psychiatry 33, 379–388.

Catani, M., Mesulam, M.M., Jakobsen, E., Malik, F., Martersteck, A., Wieneke, C., Thompson, C.K., Thiebaut de Schotten, M., Dell'Acqua, F., Weintraub, S., Rogalski, E., 2013. A novel frontal pathway underlies verbal fluency in primary progressive aphasia. Brain 136, 2619–2628.

Chen, Q., Boeve, B.F., Forghanian-Arani, A., Senjem, M.L., Jack Jr., C.R., Przybelski, S.A., Lesnick, T.G., Kremers, W.K., Fields, J.A., Schwarz, C.G., Gunter, J.L., Trzasko, J.D., Graff-Radford, J., Savica, R., Knopman, D.S., Dickson, D.W., Ferman, T.J., Graff-Radford, N., Petersen, R.C., Kantarci, K., 2021. MRI quantitative susceptibility mapping of the substantia nigra as an early biomarker for Lewy body disease. J. Neuroimaging 31, 1020–1027.

Cogswell, P.M., Wiste, H.J., Senjem, M.L., Gunter, J.L., Weigand, S.D., Schwarz, C.G., Arani, A., Therneau, T.M., Lowe, V.J., Knopman, D.S., Botha, H., Graff-Radford, J., Jones, D.T., Kantarci, K., Vemuri, P., Boeve, B.F., Mielke, M.M., Petersen, R.C., Jack Jr., C.R., 2021. Associations of quantitative susceptibility mapping with Alzheimer's disease clinical and imaging markers. Neuroimage 224, 117433.

Duffy, J.R., Josephs, K.A., 2012. The diagnosis and understanding of apraxia of speech: why including neurodegenerative etiologies may be important. J. Speech Lang. Hear Res. 55, S1518–S1522.

Dubois, B., Slachevsky, A., Litvan, I., Pillon, B., 2000. The FAB: a frontal assessment battery at bedside. Neurology 55, 1621–1626.

Ewert, S., Plettig, P., Li, N., Chakravarty, M.M., Collins, D.L., Herrington, T.M., Kuhn, A. A., Horn, A., 2018. Toward defining deep brain stimulation targets in MNI space: a subcortical atlas based on multimodal MRI, histology and structural connectivity. Neuroimage 170, 271–282.

Goetz, C.G., Tilley, B.C., Shaftman, S.R., Stebbins, G.T., Fahn, S., Martinez-Martin, P., Poewe, W., Sampaio, C., Stern, M.B., Dodel, R., Dubois, B., Holloway, R., Jankovic, J., Kulisevsky, J., Lang, A.E., Lees, A., Leurgans, S., LeWitt, P.A., Nyenhuis, D., Olanow, C.W., Rascol, O., Schrag, A., Teresi, J.A., van Hilten, J.J., LaPelle, N., Movement Disorder Society, U.R.T.F., 2008. Movement Disorder Society-sponsored revision of the Unified Parkinson's Disease Rating Scale (MDS-UPDRS): scale presentation and clinimetric testing results. Mov. Disord. 23, 2129–2170.

Golbe, L.I., Ohman-Strickland, P.A., 2007. A clinical rating scale for progressive supranuclear palsy. Brain 130, 1552–1565.

Gorno-Tempini, M.L., Dronkers, N.F., Rankin, K.P., Ogar, J.M., Phengrasamy, L., Rosen, H.J., Johnson, J.K., Weiner, M.W., Miller, B.L., 2004. Cognition and anatomy in three variants of primary progressive aphasia. Ann. Neurol. 55, 335–346.

Gorno-Tempini, M.L., Hillis, A.E., Weintraub, S., Kertesz, A., Mendez, M., Cappa, S.F., Ogar, J.M., Rohrer, J.D., Black, S., Boeve, B.F., Manes, F., Dronkers, N.F., Vandenberghe, R., Rascovsky, K., Patterson, K., Miller, B.L., Knopman, D.S., Hodges, J.R., Mesulam, M.M., Grossman, M., 2011. Classification of primary progressive aphasia and its variants. Neurology 76, 1006–1014.

Guan, X., Huang, P., Zeng, Q., Liu, C., Wei, H., Xuan, M., Gu, Q., Xu, X., Wang, N., Yu, X., Luo, X., Zhang, M., 2019. Quantitative susceptibility mapping as a biomarker for evaluating white matter alterations in Parkinson's disease. Brain Imaging Behav. 13, 220–231.

Josephs, K.A., Duffy, J.R., Strand, E.A., Whitwell, J.L., Layton, K.F., Parisi, J.E., Hauser, M.F., Witte, R.J., Boeve, B.F., Knopman, D.S., Dickson, D.W., Jack Jr., C.R., Petersen, R.C., 2006. Clinicopathological and imaging correlates of progressive aphasia and apraxia of speech. Brain 129, 1385–1398.

Josephs, K.A., Whitwell, J.L., Dickson, D.W., Boeve, B.F., Knopman, D.S., Petersen, R.C., Parisi, J.E., Jack Jr., C.R., 2008. Voxel-based morphometry in autopsy proven PSP and CBD. Neurobiol. Aging 29, 280–289.

Josephs, K.A., Duffy, J.R., Strand, E.A., Machulda, M.M., Senjem, M.L., Master, A.V., Lowe, V.J., Jack Jr., C.R., Whitwell, J.L., 2012. Characterizing a neurodegenerative syndrome: primary progressive apraxia of speech. Brain 135, 1522–1536.

Josephs, K.A., Duffy, J.R., Strand, E.A., Machulda, M.M., Senjem, M.L., Lowe, V.J., Jack Jr., C.R., Whitwell, J.L., 2013. Syndromes dominated by apraxia of speech show distinct characteristics from agrammatic PPA. Neurology 81, 337–345.

Josephs, K.A., Duffy, J.R., Strand, E.A., Machulda, M.M., Senjem, M.L., Gunter, J.L., Schwarz, C.G., Reid, R.I., Spychalla, A.J., Lowe, V.J., Jack Jr., C.R., Whitwell, J.L., 2014. The evolution of primary progressive apraxia of speech. Brain 137, 2783–2795.

Josephs, K.A., Duffy, J.R., Clark, H.M., Utianski, R.L., Strand, E.A., Machulda, M.M., Botha, H., Martin, P.R., Pham, N.T.T., Stierwalt, J., Ali, F., Buciuc, M., Baker, M., Fernandez De Castro, C.H., Spychalla, A.J., Schwarz, C.G., Reid, R.I., Senjem, M.L., Jack Jr., C.R., Lowe, V.J., Bigio, E.H., Reichard, R.R., Polley, E.J., Ertekin-Taner, N., Rademakers, R., DeTure, M.A., Ross, O.A., Dickson, D.W., Whitwell, J.L., 2021. A molecular pathology, neurobiology, biochemical, genetic and neuroimaging study of progressive apraxia of speech. Nat. Commun. 12, 3452.

Kertesz, A., 2007. Western Aphasia Battery-Revised. PsychCorp, San Antonio.

Kim, H.G., Park, S., Rhee, H.Y., Lee, K.M., Ryu, C.W., Rhee, S.J., Lee, S.Y., Wang, Y., Jahng, G.H., 2017. Quantitative susceptibility mapping to evaluate the early stage of Alzheimer's disease. Neuroimage Clin. 16, 429–438.
Lancione, M., Tosetti, M., Donatelli, G., Cosottini, M., Costagli, M., 2017. The impact of white matter fiber orientation in single-acquisition quantitative susceptibility mapping. NMR Biomed 30.
Langkammer, C., Schweser, F., Krebs, N., Deistung, A., Goessler, W., Scheurer, E., Sommer, K., Reishofer, G., Yen, K., Fazekas, F., Ropele, S., Reichenbach, J.R., 2012. Quantitative susceptibility mapping (QSM) as a means to measure brain iron? A post mortem validation study. Neuroimage 62, 1593–1599.
Lansing, A.E., Ivnik, R.J., Cullum, C.M., Randolph, C., 1999. An empirically derived short form of the Boston naming test. Arch. Clin. Neuropsychol. 14, 481–487.
Li, W., Wang, N., Yu, F., Han, H., Cao, W., Romero, R., Tantiwongkosi, B., Duong, T.Q., Liu, C., 2015. A method for estimating and removing streaking artifacts in quantitative susceptibility mapping. Neuroimage 108, 111–122.
Liu, C., Li, W., Johnson, G.A., Wu, B., 2011. High-field (9.4 T) MRI of brain dysmyelination by quantitative mapping of magnetic susceptibility. Neuroimage 56, 930–938.
Liu, C., Wei, H., Gong, N.J., Cronin, M., Dibb, R., Decker, K., 2015. Quantitative susceptibility mapping: contrast mechanisms and clinical applications. Tomography 1, 3–17.
Mazzucchi, S., Del Prete, E., Costagli, M., Frosini, D., Paoli, D., Migaleddu, G., Cecchi, P., Donatelli, G., Morganti, R., Siciliano, G., Cosottini, M., Ceravolo, R., 2022. Morphometric imaging and quantitative susceptibility mapping as complementary tools in the diagnosis of parkinsonisms. Eur. J. Neurol. 29, 2944–2955.
Nasreddine, Z.S., Phillips, N.A., Bédirian, V., Charbonneau, S., Whitehead, V., Collin, I., Cummings, J.L., Chertkow, H., 2005. The Montreal Cognitive Assessment, MoCA: a brief screening tool for mild cognitive impairment. J. Am. Geriatr. Soc. 53, 695–699.
Ravanfar, P., Loi, S.M., Syeda, W.T., Van Rheenen, T.E., Bush, A.I., Desmond, P., Cropley, V.L., Lane, D.J.R., Opazo, C.M., Moffat, B.A., Velakoulis, D., Pantelis, C., 2021. Systematic review: quantitative susceptibility mapping (QSM) of brain iron profile in neurodegenerative diseases. Front. Neurosci. 15, 618435.
Schofield, M.A., Zhu, Y., 2003. Fast phase unwrapping algorithm for interferometric applications. Opt. Lett. 28, 1194–1196.
Seckin, Z.I., Duffy, J.R., Strand, E.A., Clark, H.M., Utianski, R.L., Machulda, M.M., Botha, H., Ali, F., Thu Pham, N.T., Lowe, V.J., Whitwell, J.L., Josephs, K.A., 2020. The evolution of parkinsonism in primary progressive apraxia of speech: A 6-year longitudinal study. Parkinsonism Relat. Disord. 81, 34–40.
Sibgatulin, R., Gullmar, D., Deistung, A., Ropele, S., Reichenbach, J.R., 2021. In vivo assessment of anisotropy of apparent magnetic susceptibility in white matter from a single orientation acquisition. Neuroimage 241, 118442.
Sjostrom, H., Granberg, T., Westman, E., Svenningsson, P., 2017. Quantitative susceptibility mapping differentiates between parkinsonian disorders. Parkinsonism Relat. Disord. 44, 51–57.
Sjostrom, H., Surova, Y., Nilsson, M., Granberg, T., Westman, E., van Westen, D., Svenningsson, P., Hansson, O., 2019. Mapping of apparent susceptibility yields promising diagnostic separation of progressive supranuclear palsy from other causes of parkinsonism. Sci. Rep. 9, 6079.
Soros, P., Sokoloff, L.G., Bose, A., McIntosh, A.R., Graham, S.J., Stuss, D.T., 2006. Clustered functional MRI of overt speech production. Neuroimage 32, 376–387.
Strand, E.A., Duffy, J.R., Clark, H.M., Josephs, K., 2014. The Apraxia of Speech Rating Scale: a tool for diagnosis and description of apraxia of speech. J. Commun. Disord. 51, 43–50.
Stuber, C., Morawski, M., Schafer, A., Labadie, C., Wahnert, M., Leuze, C., Streicher, M., Barapatre, N., Reimann, K., Geyer, S., Spemann, D., Turner, R., 2014. Myelin and iron concentration in the human brain: a quantitative study of MRI contrast. Neuroimage 93 (Pt 1), 95–106.
Sun, H., Walsh, A.J., Lebel, R.M., Blevins, G., Catz, I., Lu, J.Q., Johnson, E.S., Emery, D.J., Warren, K.G., Wilman, A.H., 2015. Validation of quantitative susceptibility mapping with Perls' iron staining for subcortical gray matter. Neuroimage 105, 486–492.
Tzourio-Mazoyer, N., Landeau, B., Papathanassiou, D., Crivello, F., Etard, O., Delcroix, N., Mazoyer, B., Joliot, M., 2002. Automated anatomical labeling of activations in SPM using a macroscopic anatomical parcellation of the MNI MRI single-subject brain. Neuroimage 15, 273–289.
Utianski, R.L., Duffy, J.R., Clark, H.M., Strand, E.A., Botha, H., Schwarz, C.G., Machulda, M.M., Senjem, M.L., Spychalla, A.J., Jack Jr., C.R., Petersen, R.C., Lowe, V.J., Whitwell, J.L., Josephs, K.A., 2018a. Prosodic and phonetic subtypes of primary progressive apraxia of speech. Brain Lang. 184, 54–65.
Utianski, R.L., Whitwell, J.L., Schwarz, C.G., Senjem, M.L., Tosakulwong, N., Duffy, J.R., Clark, H.M., Machulda, M.M., Petersen, R.C., Jack Jr., C.R., Lowe, V.J., Josephs, K. A., 2018b. Tau-PET imaging with [18F]AV-1451 in primary progressive apraxia of speech. Cortex 99, 358–374.
Valls Carbo, A., Reid, R.I., Tosakulwong, N., Weigand, S.D., Duffy, J.R., Clark, H.M., Utianski, R.L., Botha, H., Machulda, M.M., Strand, E.A., Schwarz, C.G., Jack, C.R., Josephs, K.A., Whitwell, J.L., 2022. Tractography of supplementary motor area projections in progressive speech apraxia and aphasia. Neuroimage Clin. 34, 102999.
Wang, Y., Liu, T., 2015. Quantitative susceptibility mapping (QSM): Decoding MRI data for a tissue magnetic biomarker. Magn. Reson. Med. 73, 82–101.
Wang, Y., Spincemaille, P., Liu, Z., Dimov, A., Deh, K., Li, J., Zhang, Y., Yao, Y., Gillen, K. M., Wilman, A.H., Gupta, A., Tsiouris, A.J., Kovanlikaya, I., Chiang, G.C., Weinsaft, J.W., Tanenbaum, L., Chen, W., Zhu, W., Chang, S., Lou, M., Kopell, B.H., Kaplitt, M.G., Devos, D., Hirai, T., Huang, X., Korogi, Y., Shtilbans, A., Jahng, G.H., Pelletier, D., Gauthier, S.A., Pitt, D., Bush, A.I., Brittenham, G.M., Prince, M.R., 2017. Clinical quantitative susceptibility mapping (QSM): Biometal imaging and its emerging roles in patient care. J. Magn. Reson. Imaging 46, 951–971.
Watkins, K.E., Smith, S.M., Davis, S., Howell, P., 2008. Structural and functional abnormalities of the motor system in developmental stuttering. Brain 131, 50–59.
Whitwell, J.L., Master, A.V., Avula, R., Kantarci, K., Eggers, S.D., Edmonson, H.A., Jack Jr., C.R., Josephs, K.A., 2011. Clinical correlates of white matter tract degeneration in progressive supranuclear palsy. Arch. Neurol. 68, 753–760.
Whitwell, J.L., Duffy, J.R., Strand, E.A., Machulda, M.M., Senjem, M.L., Gunter, J.L., Kantarci, K., Eggers, S.D., Jack Jr., C.R., Josephs, K.A., 2013a. Neuroimaging comparison of primary progressive apraxia of speech and progressive supranuclear palsy. Eur. J. Neurol. 20, 629–637.
Whitwell, J.L., Duffy, J.R., Strand, E.A., Xia, R., Mandrekar, J., Machulda, M.M., Senjem, M.L., Lowe, V.J., Jack Jr., C.R., Josephs, K.A., 2013b. Distinct regional anatomic and functional correlates of neurodegenerative apraxia of speech and aphasia: an MRI and FDG-PET study. Brain Lang. 125, 245–252.
Whitwell, J.L., Lowe, V.J., Tosakulwong, N., Weigand, S.D., Senjem, M.L., Schwarz, C.G., Spychalla, A.J., Petersen, R.C., Jack Jr., C.R., Josephs, K.A., 2017. [(18) F]AV-1451 tau positron emission tomography in progressive supranuclear palsy. Mov. Disord. 32, 124–133.
Wu, B., Li, W., Guidon, A., Liu, C., 2012. Whole brain susceptibility mapping using compressed sensing. Magn. Reson. Med. 67, 137–147.